Three-dimensional structure in a crystallized dusty plasma

J. B. Pieper, J. Goree,* and R. A. Quinn

Department of Physics and Astronomy, The University of Iowa, Iowa City, Iowa 52242

(Received 24 January 1996; revised manuscript received 8 July 1996)

Direct imaging of the three-dimensional structure of a system of particles suspended in a dusty plasma reveals coexisting bcc and simple-hexagonal crystal structures. The coexistence is attributed to a bistability which appears in a recent theory predicting an attractive region in the plasma downstream of a particle in an ion flow. Both structures are polycrystalline, and they have short-range translational but quasi-long-range orientational order within a grain. This ordering is characteristic of the two-dimensional hexatic phase, but the existence of grain boundaries is not. [S1063-651X(96)10611-5]

PACS number(s): 52.25.Vy, 82.70.Dd

I. INTRODUCTION

The recently discovered Coulomb crystallization of micrometer-size particles in a laboratory plasma [1–6] holds great potential as a model system for studies of structure, dynamics, and phase transitions in condensed matter. This makes the topic of dusty plasmas of interest to a wide community of researchers. In common low-density laboratory plasmas, large (≈ 10 μm) particles charge typically to $\sim -10^4 e$, so that they can be electrically levitated in a few horizontal planes directly above a horizontal negatively biased electrode. They interact through their repulsive Coulomb potential, which is screened by ions and electrons in the plasma. The particle system crystallizes when the nearest-neighbor potential energy is large compared to the particle thermal energy, as can be accomplished by using large particles and cooling them by drag on a neutral gas background.

Most experimenters [3–6] have reported observing particles arranged in the simple-hexagonal structure, where the particles are arranged on a triangular lattice in a horizontal plane with one particle directly above another in the vertical direction. Chu and I have reported bcc and fcc structures coexisting in a dusty plasma under one set of operating conditions, and the simple-hexagonal structure under another set [1]. These reports are based on their visual observations of various lattice planes coming into view while adjusting their microscope focus, which they interpreted by sketching the three-dimensional (3D) unit cells.

In this paper we report the first direct 3D images of the bcc and simple-hexagonal structures in a dusty plasma, using a technique which permits selective imaging of crystal planes lying well inside the crystal surface. Similar depth-resolved imaging methods have been developed recently for colloidal crystals at low volume fractions ($\geqslant 0.1\%$) by using confocal scanning laser microscopy [7]. The dusty plasma system has the advantage of a much lower volume fraction ($\approx 0.01\%$), potentially allowing the imaging of a much larger number of parallel crystal planes.

The ability to record a three-dimensional image of par-

ticles in a plasma is new. Plasma diagnostics generally provide measures of continuum quantities, such as number density or velocity distribution functions, which average out much of the discrete nature of the particles themselves, whether they are electrons or ions. In most plasma experiments, it is impractical to measure individual particles, and it is most certainly impractical to measure the positions of all of them in an extended sample volume. However, in a dusty plasma, large (≈ 10 μm) particles scatter light efficiently, and it is possible to image them directly. Here we develop this direct imaging into a 3D analysis tool.

In our images the 3D arrangement of the particles is clearly evident. The bcc and simple-hexagonal structures coexist within the same suspension. Static structural analysis of the images reveal that both structures are polycrystalline, with defects concentrated along grain boundaries, and they both have quasi-long-range orientational order within a grain but only short-range translational order. The coexistence of the two structures lends support to recent theoretical studies [8,9] suggesting that the equilibrium structure is bistable due to an anisotropy in the interparticle potential, caused by the rapid flow of ions toward the electrode.

II. EXPERIMENT

Our 3D imaging was done by assembling a stack of images of horizontal planes within the volume of the particle suspension, each plane being illuminated with a focused horizontal laser sheet. The sheet was focused to a Gaussian full width of ≈ 90 μm, which is smaller than the particle spacing and allows resolution of individual crystal planes. Both the sheet and a high-resolution video camera that was focused upon it were moved together vertically, maintaining the focus. This was done in 30-μm steps to scan through the 3D sample volume. Each horizontal image in this stack was digitized, and the brightness data were assembled into a single set which could be displayed as volumetric data. Bilinear interpolation allowed us to produce images on arbitrarily oriented cross-section planes within the sample volume, which we chose to align with the vertical {110} lattice planes.

A 1.4-torr krypton plasma was formed by applying a 13.56-MHz radio-frequency (rf) voltage to an Al electrode with a depression 1.5 mm deep and ~ 6 cm in diameter. The

---
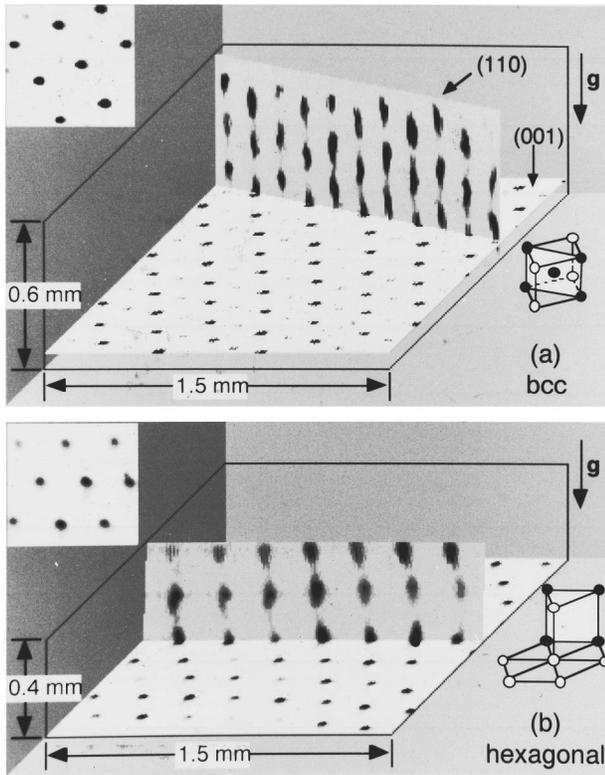
FIG. 1. Images within a 3D volume of Coulomb crystals formed by 9.4-μm-diam polymer spheres in a 1.4-torr Kr discharge. In each image one horizontal plane and a vertical cross section through the data are shown; the inset shows a portion of the horizontal plane viewed from above. The data are contained in a stack of horizontal planar images resolved by selective illumination by a 90-μm-thick sheet of light from a focused, swept laser beam. The particle images appear longer in the vertical direction due to the infinite thickness of the laser sheet. (a) bcc, (b) simple-hexagonal structure.

rf power deposited in the plasma was 2.3 W, the peak-to-peak and dc self-bias voltages were 200 and -43 V, respectively. Polymethylene melamine spheres of diameter 9.4 ± 0.3 μm were introduced into the glow, where they formed a 2-mm-thick cloud suspended 2 mm above the depressed electrode surface. The depression helped confine a larger number of horizontal layers, which we found necessary to obtain bcc structures. Using a passively filtered Langmuir probe inserted in the middle of the particle cloud, we found the plasma electron temperature was 8.1 eV. The density from the probe characteristic was 1.8×10^9 and 3.2×10^8 cm^{-3} as determined by electron and ion saturation currents, respectively, where the Allen, Boyd, and Reynolds (ABR) analysis was used for the latter. We have no explanation for the discrepancy of these two density measurements. Further details of the apparatus are given elsewhere [10].

The 3D images in Fig. 1 reveal structures that are (a) bcc with a $\langle 100 \rangle$ axis in the vertical direction, and (b) simple hexagonal in which particles are vertically aligned. Both were obtained in the same experiment, at locations a few mm apart and about halfway between the cloud's center and edge. In both cases, the particle spacing Δ in the horizontal plane is 195 ± 1 μm. The bcc structure is oriented differently from that of Chu and I, who found a vertical $\langle 110 \rangle$ axis [1].
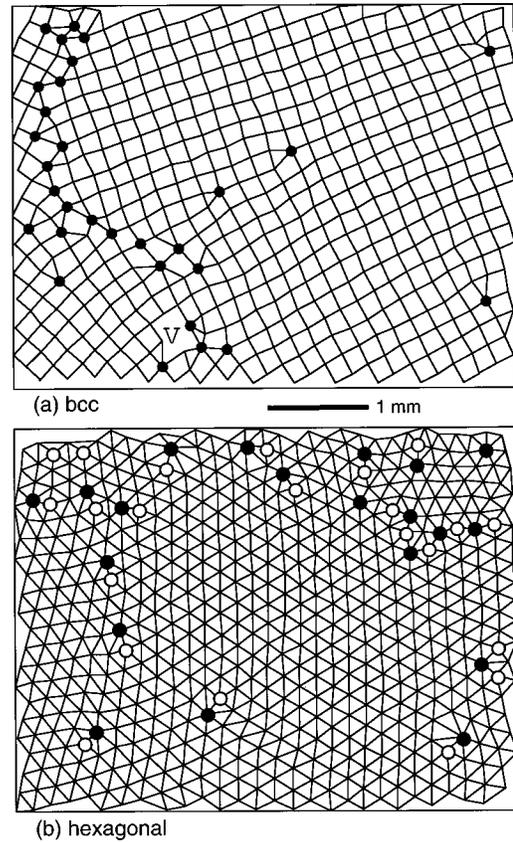
FIG. 2. Defect maps for one horizontal plane of the crystals of Fig. 1, constructed from Delaunay triangulations. Each vertex represents a particle position; the segments represent nearest-neighbor bonds. (a) Plane 6 (numbered from top of cloud) of bcc crystal: ●, dislocation; V, vacancy. (b) Plane 1 of simple-hexagonal crystal, vertices marked for number of nearest neighbors: ○, 5; unmarked, 6; ●, ≥ 7. Dislocations consist of ○-● pairs.

We analyzed images of the horizontal crystal planes using two-dimensional static structural methods. In-plane nearest-neighbor bonds were identified by Delaunay triangulation. For the {100} planes of the bcc structure, we deleted the longest side of each Delaunay triangle, leaving the particles connected by a quadrilateral network except at defect sites. Defect analyses of the bond networks are shown for one plane of each crystal in Fig. 2. Note that both the bcc and simple-hexagonal structures are polycrystalline, with dislocation groups arranged on grain boundaries, and that there are also unbound dislocations and vacancies. When comparing defect maps of different planes within a crystal, we observed a tendency toward vertical alignment of similar defects in adjacent planes.

The degree of order in the observed structures was characterized by the translational and bond-orientational correlation functions, $g_G(|\mathbf{r} - \mathbf{r}'|) = \langle \exp[i\mathbf{G}_0 \cdot (\mathbf{r} - \mathbf{r}')] \rangle$ and $g_n(|\mathbf{r} - \mathbf{r}'|) = \langle \exp\{in[\theta(\mathbf{r}) - \theta(\mathbf{r}')]\} \rangle$, respectively. We also calculated the structure factor $S(k)$. The calculations followed the procedures in Ref. [11] with the following differences. The function $g_n(r)$ was calculated with $n=6$ for the hexagonal structure and $n=4$ for the cubic. In $g_G(r)$, $\mathbf{G}_0$ is the shortest reciprocal lattice vector associated with the structure, i.e., $S(k)$ has its first peak at $k=G_0$. From the n

possible directions for $\mathbf{G}_0$, we chose the one that maximized the average of $\exp[i\mathbf{G}_0 \cdot (\mathbf{r} - \mathbf{r}')]$ over the n nearest neighbors of the particle at $\mathbf{r}$. Both correlation functions were fit by exponential decays with distance, $g_G(r) \propto \exp(-r/\xi)$ and $g_n(r) \propto \exp(-r/\xi_n)$, yielding correlation lengths ξ and ξ_n; we also fit g_n by the power-law form $g_n(r) \propto r^{-\eta}$.

III. BISTABILITY

An explanation is needed for our observation of coexisting hexagonal and square lattices in the same plasma. We attribute this to a bistable equilibrium. Explaining this requires reviewing the reason the simple-hexagonal structure is stable.

Several experimenters have reported seeing the simple-hexagonal structure, but were unable to explain it [1,4,6]. It was a surprising finding, because that structure is not a minimum energy state for an isotropic interparticle potential. Apparently the particles interact anisotropically. In experiments, the vertical direction is distinguished by the sheath electric field, ion flow, and gravity, all pointing toward the electrode. Some experimenters have suggested that gravity should be considered in explaining the simple-hexagonal structure; however, it is the plasma and not gravity that determines the interparticle potential and whether it is isotropic. We attribute the structure to the ion flow, which is supersonic in the sheath. Recent independent theoretical studies by Vladimirov and Nambu [8] and Melandsø and Goree [9] have shown that in an otherwise uniform plasma, the flow leaves a polarized wake behind a particle, with ions focusing to make the plasma potential positive in a local region. This positive region, which is typically four Debye lengths downstream of the particle [9], will attract negative particles, promoting the vertical alignment observed experimentally in the simple-hexagonal structure.

The equilibrium we observed is bistable because there are two crystalline configurations that minimize the potential energy with respect to a small displacement in particle position. The simple-hexagonal structure reduces the potential energy by bringing particles into the attractive potential of the ion focus created by the particle above it. The square bcc lattices on the other hand have particles arranged not one on top of another but staggered, minimizing the repulsive part of the potential. Both are stable and can coexist, but the one that is favored energetically is more likely to be observed. This will depend on the depth of the ion focus potential, which in turn will depend on the plasma conditions.

This argument is supported qualitatively by a 2D simulation reported recently by Melandsø and Goree [12], who followed the motion of many particles beginning at random positions in a sheath, and used a self-consistent electric potential. Comparing experiment and simulation is limited because the simulation was two dimensional, assuming infinite cylindrical particles. The simulation assumed a plasma density of 1×10^8 cm^{-3} and an ion speed equal to twice the acoustic speed (which is believed to be a typical value inside the sheath edge for our type of plasma). The particles settled in one of two stable equilibria: a vertically aligned equilibrium (roughly corresponding to the experimentally observed simple hexagonal) or a staggered vertical arrangement (roughly analogous to close-packed structures such as the experimental bcc). The equilibrium that was more probable was found to be the one with the lower potential energy, as one might expect, and that was found to depend on the particle charge-to-mass ratio q/m and on $\kappa \equiv \Delta/\lambda_D$, the ratio of the particle spacing to Debye length. Larger values of q/m and smaller values of κ tended to favor the vertically aligned arrangement.

In experimental tests, we found a transition between the simple-hexagonal and the bcc structures. When the rf voltage was suddenly increased by 3 dB, a predominately bcc cloud rearranged itself in a few seconds to become simple hexagonal, with the in-plane particle spacing Δ remaining very nearly constant. A higher rf voltage and power has the effect of reducing the Debye length λ_D, which in turn increases κ for a constant Δ. It also caused the floating potential to become more negative compared to the plasma potential, as measured using a Langmuir probe in the middle of the dust layer. This should correspond to a larger (more negative) charge-to-mass ratio on a particle. With our present instrumentation, we are unable to determine how the ion drift speed in the sheath depends on the rf power. Theory predicts an increasing flow speed would cause the attractive potential region to extend farther downstream from a particle [9].

A close comparison with the simulation results of Ref. [12] is not suitable because the simulation was carried out in 2D. It is interesting, however, that we found that the vertically aligned structure was more probable at a higher charge-to-mass ratio as predicted by the simulation, but also more probable at a higher value of κ, in apparent contradiction to the simulation. This points to a need for 3D simulations for more direct comparisons.

Simulations of isotropic Yukawa systems have shown a transition between stable bcc and fcc, with bcc favored for $\kappa < 5$ at the melting transition and $\kappa < 1.72$ at zero temperature [13]. Quantitative comparison of our results with this simulation is hampered by the ambiguity of the Debye length λ_D in a flowing plasma due to the anisotropic wake potential [9] and the inconsistency of our two density measurements. The anisotropy in the experiments allows the existence of the stable simple-hexagonal structure which does not appear in the isotropic Yukawa simulations. Unlike Chu and I [1], we did not see the bcc-fcc transition, perhaps because our κ or charge-to-mass ratio was different.

IV. STRUCTURES

An indication of how highly ordered a structure is can be found from static structural analysis. Here we present calculations of correlation functions and structure factors on a horizontal plane, and how these results varied with height in the particle cloud.

We calculated the correlation functions g_G and g_n for each horizontal plane in the sample volume and then averaged them. The results are shown in Figs. 3 and 4, respectively. Both structures have short-range transitional order, with the average in-plane correlation length $\xi = (3.6 \pm 0.2)\Delta$ for the bcc structure and $\xi = (3.0 \pm 0.2)\Delta$ for hexagonal. The fitting to the orientational function g_n is good up to an abrupt change in the slope at radii of 10Δ to 15Δ. This is comparable to the radius of polycrystalline grains, as seen in Fig. 3. For the parts of the data which are fit well by
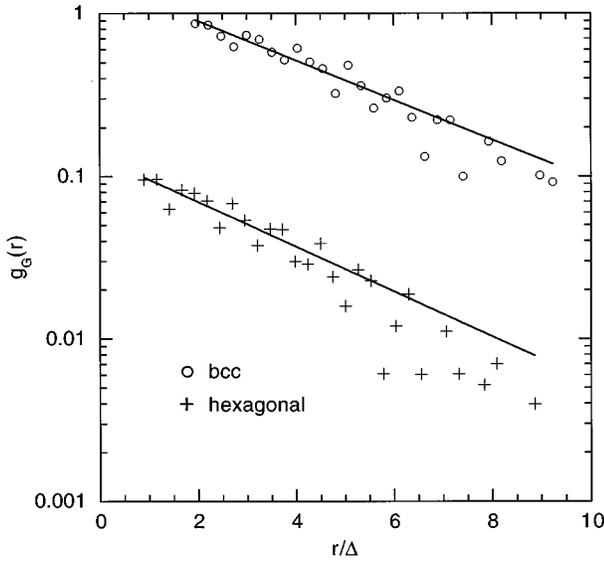
FIG. 3. The translational order-parameter correlation function $g_G(r)$ for the bcc and simple-hexagonal crystals of Fig. 1, calculated in each horizontal plane and averaged over planes. The curves are fits by decaying exponentials which yield correlation lengths (in units of particle separation Δ) $\xi/\Delta = 3.6 \pm 0.2$ for bcc and $\xi/\Delta = 3.0 \pm 0.2$ for hexagonal.

the curves, we determined average orientational correlation lengths $\xi_4/\Delta = 116 \pm 4$ for the bcc structure and $\xi_6/\Delta = 17.9 \pm 0.5$ for the hexagonal, and power-law exponents $\eta = 0.050 \pm 0.005$ for bcc and $\eta = 0.20 \pm 0.01$ for hex-
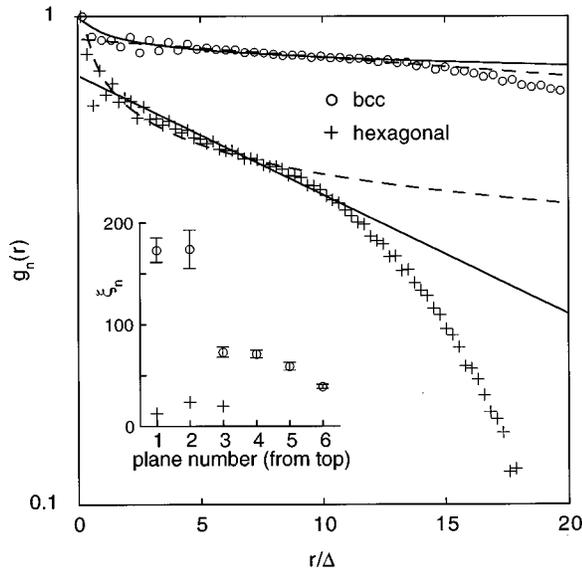
FIG. 4. The bond-orientational correlation function $g_n(r)$ for the bcc and simple-hexagonal crystals of Fig. 1, calculated in each horizontal plane and averaged over planes. The exponential fits (solid curves) yield values of the correlation length $\xi_4/\Delta = 116 \pm 4$ (bcc) and $\xi_6/\Delta = 17.9 \pm 0.5$ (hexagonal). The power-law fits (dashed curves) yield $\eta = 0.050 \pm 0.005$ (bcc) and $\eta = 0.20 \pm 0.01$ (hexagonal). The inset shows the fit values of ξ_n in the individual planes. The fits were calculated only for $r \leqslant 15\Delta$ for bcc crystal and $r \leqslant 10\Delta$ for hexagonal.
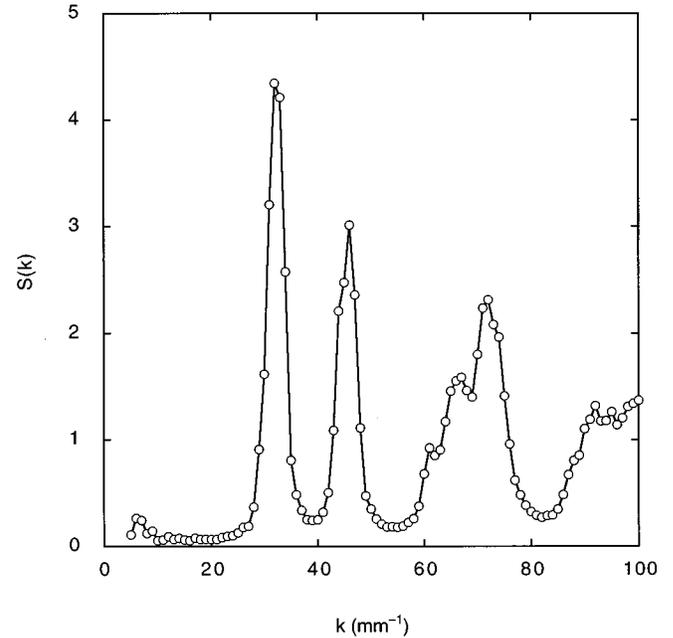
FIG. 5. The structure factor $S(k)$ for the bcc crystal, calculated in each {100} plane and averaged over planes.

agonal. The correlation functions for the individual crystal planes revealed that the uppermost planes of the bcc crystal are the most orientationally ordered, with ξ_n decreasing as one moves down toward the electrode. By contrast, the translational order does not vary significantly with height within the regions studied.

The structure factor $S(k)$ in Fig. 5 is another useful measure of ordering. The height of its first peak, $S(G_0)$, is a common measure of the freezing point. The empirical criterion of Hansen and Verlet [14] specifies $S(G_0) = 2.85$ at freezing in 3D systems, while for 2D systems a value of 5.75 was predicted by Ramakrishnan's [15] first-order freezing theory. Our calculated $S(G_0)$, averaged over the {100} planes of our bcc crystal, is close to 4.4, and it reaches 4.9 in three of the planes. We also found that the peak was doubled in the upper planes of the crystal, with a maximum splitting of about 1.8 mm^{-1}. The splitting decreased toward the electrode until only one peak was resolved in the lowest two planes. We examined the non-angle-averaged function $S(\mathbf{k})$, and found that the splitting was between peaks separated by 90° in $\mathbf{k}$ space. This indicates that the square lattice in the upper {100} planes is compressed by about 5% in the [100] direction compared to the [010] direction, and this deformation gradually disappears as we move down toward the electrode. This may be due to surface effects, because the sample location was not in the lateral center of the cloud but toward one edge. We have observed, however, that the orientation of the local crystal axes is not affected by proximity to the edge of the trapping region above the electrode except within a few particle spacings of the edge, and therefore expect that the effect on the ordering itself is negligible.

The short range of translational order in our observed structures is very atypical of "real" 2D or 3D solids, but fits well with the idea of the 2D "hexatic" phase of Kosterlitz-Thouless-Halperin-Nelson-Young (KTHNY) theory [16–18] when compared with the much longer range of orientational

order. The values of η obtained by curve fitting are consistent with the prediction $0<\eta<1/4$ for the hexatic phase. However, the presence of grain boundaries, which are arrays of bound dislocations, is not consistent with the KTHNY theory, in which the solid-to-hexatic transition is mediated by the unbinding of such structures into a gas of free dislocations.

V. CONCLUSIONS

We have made a direct determination of the 3D structure of a plasma dust crystal, including direct 3D images and structural analysis in a 3D volume. We find bcc and simple-hexagonal structures which can coexist stably within a dust cloud, and have observed a transition between the two structures when the plasma conditions are varied. The two structures are bistable, and we found that the simple-hexagonal structure is more probable at larger values of κ and the charge-to-mass ratio. The two structures we observed have comparable degrees of ordering in the horizontal plane, and resemble the intermediate hexatic phase of KTHNY theory in the plane except for the polycrystallinity of the structures, which is not consistent with that theory.

It should be possible to extend the method of 3D imaging we have described here to imagine a volume sample that is more extended in the vertical direction than can be achieved in the laboratory experiments we have reported here. The low volume fraction of the dusty plasma should allow up to 500 particle layers to be imaged. Such a thick particle cloud might be achieved by carrying out the experiments under microgravity conditions. This experimental approach will be explored in the future. Moreover, our results indicate a need for 3D simulations of particle motion and a need to understand the anisotropic interaction potential in three dimensions. An understanding of the potential between dust particles in the anisotropic sheath region should also give insight into the dynamics of dust crystals, which are currently under investigation [19].

ACKNOWLEDGMENTS

[1] J. H. Chu and Lin I, Phys. Rev. Lett. **72**, 4009 (1994).

[2] J. H. Chu and Lin I, Physica A **205**, 183 (1994).

[3] H. Thomas *et al.*, Phys. Rev. Lett. **73**, 652 (1994).

[4] Y. Hayashi and K. Tachibana, Jpn. J. Appl. Phys. **33** 804 (1994).

[5] A. Melzer, T. Trottenberg, and A. Piel, Phys. Lett. A **191**, 31 (1994).

[6] T. Trottenberg, A. Melzer, and A. Piel, Plasma Sources Sci. Technol. **4**, 450 (1995).

[7] N. A. M. Verhaegh *et al.*, J. Chem. Phys. **102**, 1416 (1995).

[8] S. V. Vladimirov and M. Nambu, Phys. Rev. E **52**, R2172 (1995).

[9] F. Melandsø and J. Goree, Phys. Rev. E **52**, 5312 (1995).

[10] J. B. Pieper, J. Goree, and R. A. Quinn, J. Vac. Sci. Technol. A **14**, 519 (1996).

[11] R. A. Quinn *et al.*, Phys. Rev. E **53**, R2049 (1996).

[12] F. Melandsø and J. Goree, J. Vac. Sci. Technol. A **14**, 511 (1996).

[13] M. O. Robbins, K. Kremer, and G. S. Grest, J. Chem. Phys. **88**, 3286 (1988).

[14] J.-P. Hansen and L. Verlet, Phys. Rev. **184**, 151 (1969).

[15] T. V. Ramakrishnan, Phys. Rev. Lett. **48**, 541 (1982).

[16] J. M. Kosterlitz and D. J. Thouless, J. Phys. C **6**, 1181 (1973).

[17] B. I. Halperin and D. R. Nelson, Phys. Rev. Lett. **41**, 121 (1978).

[18] A. P. Young, Phys. Rev. B **19**, 1855 (1979).

[19] J. B. Pieper and J. Goree, Phys. Rev. Lett. (to be published).